

Magnetic damping losses of tipped cantilevers

Moresi Giorgio¹, Beat Meier¹, Richard Magin² and Ernst Meyer³

¹ Laboratory of Physical Chemistry, ETH Zürich, Hönggerberg HCI D231 CH-8093 Zürich, Switzerland

² Department of Bioengineering, University of Illinois at Chicago, Science and Engineering Office Building (M/C 063), 851 South Morgan, Chicago, IL 60607-7052, USA

³ Department of Physic and Astronomy, University of Basel, Klingelbergstrasse 82, CH-4056 Basel, UK

Received 30 August 2005, in final form 12 December 2005

Published 16 January 2006

Online at stacks.iop.org/Nano/17/871

Abstract

In magnetic resonance force microscopy single spin experiments, forces in the attonewton range have to be measured. Non-commercial, soft single crystalline silicon bar cantilevers with a high quality factor and minimized spring constants have to be used, in order to improve the detection sensitivity. In our low temperature force microscope we obtain force sensitivities of the order of 10^{-18} N Hz^{-1/2} at 10 K (Gysin 2002 Temperaturverhalten der Elastizität und inneren Reibung mikromechanischer Resonatoren, *Thesis* Basel).

Micrometre-sized magnetic particles, which generate a magnetic field of 500 G and magnetic field gradients ($dB/dz \gg 1$ G nm⁻¹), are attached on ultrasensitive cantilevers. A severe loss in force sensitivity and a frequency shift are observed while exposing a cantilever with a magnetic tip to a homogeneous magnetic field. To minimize the damping losses of the cantilevers with ferromagnetic particles, various magnetic materials (e.g. SmCo₅, Nd₂Fe₁₄B, and Pr₂Fe₁₄B) with different grain and domain sizes are investigated. The lowest magnetic dissipation is observed with SmCo₅ and Pr₂Fe₁₄B tips. We try to explain the dissipation effect of cantilevers with magnetic tips.

(Some figures in this article are in colour only in the electronic version)

Introduction: damping losses of cantilevers in an external magnetic field

Magnetic losses in micrometre-size ferromagnets are of fundamental interest for data storage, for spintronics and quantum computing. A particular application is magnetic resonance force microscopy (MRFM), demanding low thermomagnetic fluctuations which perturb the spin relaxation rate of the sample and the sensitivity of the mechanical detector [2]. In order to study the thermo-fluctuation of the magnetization the cantilever magnetometry is chosen for its ability to indirectly measure the magnetization in a broad temperature and magnetic field range.

In this work we measure and study the average magnetization of hard multigrain magnetic materials like SmCo₅, Nd₂Fe₁₄B, and Pr₂Fe₁₄B and we correlate the losses with the frequency oscillations of the mechanical detector and with the static homogeneous field.

1. Theory: interaction between magnetic tip and external magnetic field

The interaction between a magnetic particle and a homogeneous magnetic field can be measured by the frequency shift induced on a mechanical lever. The frequency shift induced by the interaction with the static magnetic field can be calculated from the torque acting on the particle. Figure 1 sketches the interaction between a tipped cantilever and an external magnetic field. In order to calculate the torque acting on the cantilever the total potential energy of the mechanical resonator in an external magnetic field is minimized. The total potential energy is

$$E(\theta, \theta_m) = E_{Zeeman}(\theta, \theta_m) + E_{Spring}(\theta) + E_{Anisotropy}(\theta_m). \quad (1)$$

The total potential energy of the mechanical oscillator can be calculated from three main terms [2]: the Zeeman energy

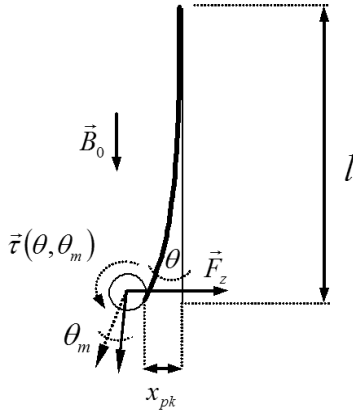


Figure 1. Tipped cantilever in a magnetic field. The sketch represents the cantilever with the magnetic particle subjected to the external magnetic field. The magnetic particle exercises a lateral force on the mechanical resonator, causing an increase in the resonance frequency. A momentum at the end of the cantilever will cause a reduction of the resonance frequency. The parameters are: l , the length of the cantilever; x_{pk} , the peak amplitude; F_z , the lateral force; θ , the angle of oscillation; θ_m , the angle of the magnetization rotation.

term, the potential energy of the spring and the anisotropy term (we neglect the exchange energy). The Zeeman energy is

$$E_{\text{Zeeman}}(\theta, \theta_m) = -M_s V B \cos(\theta - \theta_m) \quad (2)$$

where M_s is the magnetization, V the volume, B the magnetic field, θ the cantilever deflection angle and $\theta - \theta_m$ the angle between the magnetization of the tip particle and the external magnetic field.

The energy potential of the cantilever is given by

$$E_{\text{Spring}}(\theta) = \frac{1}{2} k_0 (l\theta)^2 \quad (3)$$

where k_0 is the spring constant, l the length of the cantilever and θ the deflection angle represented in figure 1.

The shape anisotropy energy in a magnetic material where the grain size is smaller than the critical size of a single magnetic domain is [3]

$$E_{\text{Anisotropy}}(\theta_m) = \mu_0 (M_s V)^2 \frac{D_{\parallel} \cos^2(\theta_m) + D_{\perp} \sin^2(\theta_m)}{2V} \quad (4)$$

where μ_0 is the magnetic permeability in vacuum, and D_{\parallel} and D_{\perp} the principal values of the demagnetization factor of a prolate spheroid parallel and perpendicular with respect to the long axis.

When the grain size has the same dimension as that of a magnetic domain the anisotropy term reduces to the magnetocrystalline anisotropy (values reported in table 1).

In other words, the expression of the anisotropy depends on the magnetocrystalline symmetry. The simple anisotropy expression (5) is widely used, but sometimes it is necessary to take high order anisotropy constants into consideration [4].

$$E_{\text{Anisotropy}}(\theta_m) = K_1 V \sin^2(\theta_m). \quad (5)$$

The anisotropy term can be distinguished between the macroscopic shape anisotropy important in small aspherical

particles and the magnetocrystalline anisotropy, which is an intrinsic lattice property. The single domain radius R_s is of the order of $0.2 \mu\text{m}$ in a modern permanent magnet. Consequently a magnetic particle larger than $1 \mu\text{m}$ is multidomain.

To calculate the anisotropy rotation angle θ_m we minimize the potential energy. The solution is calculated for the geometric anisotropy and for the magnetocrystalline anisotropy.

$$\frac{\partial E(\theta, \theta_m)}{\partial \theta_m} = 0. \quad (6)$$

For small angles ($\sin(\theta) \approx \theta$ and $\cos(\theta) \approx 1$) we find

$$\theta_m = \begin{cases} \frac{B}{B + \mu_0 M_s (D_{\perp} - D_{\parallel})} \theta & \text{(geometric anisotropy)} \\ \frac{B}{B + \frac{2K_1}{M_s}} \theta & \text{(crystalline anisotropy)}. \end{cases} \quad (7)$$

The torque $\vec{\tau}(\theta, \theta_m)$ acting on the cantilever can be calculated using the first derivative of the total energy. By minimizing the interaction with the magnetic field and replacing θ_m with the equation (7) we obtain

$$\|\vec{\tau}(\theta)\| = -\frac{\partial E(\theta)}{\partial \theta}. \quad (8)$$

Assuming small angles, the torque [2, 3] can be described by the following relation:

$$\begin{aligned} \|\vec{\tau}(\theta)\| &= -\|\vec{\tau}_{\text{mc}}(\theta) + \vec{\tau}_{\text{imc}}(\theta)\| = (\tau_{\text{mc}} + \tau_{\text{imc}})\theta \\ &\quad - \left(\frac{B\mu_0 M_s^2 (D_{\perp} - D_{\parallel}) V}{B + \mu_0 M_s (D_{\perp} - D_{\parallel})} + k_0 l^2 \right) \theta \\ &= - \left(\frac{2BK_1 V}{B + \frac{2K_1}{M_s}} + k_0 l^2 \right) \theta. \end{aligned} \quad (9)$$

The torque is then divided into two terms, the magnetic torque $\vec{\tau}_{\text{mc}}$ that interacts with the magnetic field, and the torque independent of the magnetic field $\vec{\tau}_{\text{imc}}$. The torque independent of the magnetic field is mainly due to the elasticity of the cantilever. Consequently it can be neglected when studying tip-magnetic-field interaction.

1.1. Frequency shift and damping factor

The torque acting on the cantilever induces a frequency shift. This is measured by standard FM-detection: a lock-in amplifier, a frequency counter or a phase lock loop called PLL. The frequency shift and the damping factor can be calculated with the motion equation of a damped harmonic oscillator excited at constant amplitude.

$$m\ddot{x} + \Gamma\dot{x} + k_0 x + \frac{\tau_{\text{mc}}\theta}{l} = A \sin(\omega t) \quad (10)$$

where m is the mass, Γ is the damping factor, k_0 the spring constant, l the length of the cantilever and A the exciting amplitude. From equation (10), the mechanical resonance frequency of a weak damping harmonic oscillator is

$$\omega = \sqrt{\frac{k_0}{m} + \frac{\Delta k}{m}} = \sqrt{\frac{\tau_{\text{imc}}}{ml^2} + \frac{\tau_{\text{mc}}}{ml^2} - \left(\frac{\Gamma}{2m}\right)^2} \quad (11)$$

Table 1. Magnetic properties. The table summarizes and compares the magnetic saturation, the coercivity, the Curie temperature, the anisotropy constant and the maximal radius for a monodomain of different magnetic materials.

Substance	$\mu_0 M_s$ (T)	$\mu_0 H_0$ (T)	T_c (K)	K_1 (M J m ⁻³)	K_2 (M J m ⁻³)	R_{sd} (nm)	Structure
SmCo ₅	1.07	40	1020	17.2		764	Hexagonal
Sm ₂ Co ₁₇	1.22		1190	3.3			Rhombohedral
Nd ₂ Fe ₁₄ B	1.61	7.6	585	4.9	0.65	107	Tetragonal
Pr ₂ Fe ₁₄ B	1.55		565	5		100	Tetragonal
YCo ₅	1.06		987	6.5			
Fe	2.15	0.06		0.048	0.015	6	Uniaxial
Co	1.81	0.76		0.53	0	34	
Ni	0.62	0.03		-0.005	0.005	16	Uniaxial

where the change of the spring constant is Δk . The frequency shift can then be calculated with the Taylor approximation:

$$\Delta\omega = \omega - \omega_0 = \omega_0 \left(\sqrt{1 + \frac{\frac{\tau_{mc}}{m l^2} - \left(\frac{\Gamma}{2m}\right)^2}{\omega_0^2}} - 1 \right) \cong \omega_0 \frac{1}{2} \frac{\frac{\tau_{mc}}{m l^2} - \left(\frac{\Gamma}{2m}\right)^2}{\omega_0^2}. \quad (12)$$

Finally, it is possible to compact the relation to

$$\frac{\Delta\omega}{\omega_0} = \frac{1}{2} \frac{\Delta k}{k_0} \quad (13)$$

and calculate the relation between frequency shift and magnetic field [2, 3, 5].

$$\Delta\omega = \frac{1}{2} \frac{\omega_0}{k_0} \Delta k = \frac{\omega_0}{2k_0} \left(\frac{1}{l^2} \frac{B\mu_0 M_s^2 (D_\perp - D_\parallel) V}{B + \mu_0 M_s (D_\perp - D_\parallel)} - \frac{\Gamma^2}{4m} \right) \quad (14)$$

$$\frac{\omega_0}{2k_0} \left(\frac{1}{l^2} \frac{2BK_1 V}{B + \frac{2K_1}{M_s}} - \frac{\Gamma^2}{4m} \right).$$

For large anisotropy constant ($K_1 \gg BM_s$) the frequency shift should have a linear relation with the magnetic field. At higher magnetic field the frequency shift should tend asymptotically to a constant value ($\omega_0 K_1 V / (k_0 l^2)$). The first relation of equation (14) depends on the geometry factor and it must be used for isotropic multidomain samples or soft materials. The second relation is directly correlated with the anisotropic constant of the magnetic domain. Consequently, this relation must be used for hard magnetic monodomains. Also, the damping factor Γ can induce an effect on the frequency shift.

1.2. The energy losses and the damping factor

In the previous section we have developed the relation that connects the magnetic field to the frequency shift. In this section we explain the damping factor that appears in the frequency shift relation. The damping factor comprises many independent mechanisms, which cause a loss of energy in the system.

One such loss is the thermoelastic relaxation [1]. The energy loss is caused by a delay of the elastic process between two points of the mechanical oscillator causing an irreversible process of energy loss. Experimental results show that the thermoelastic process is independent of the applied magnetic field.

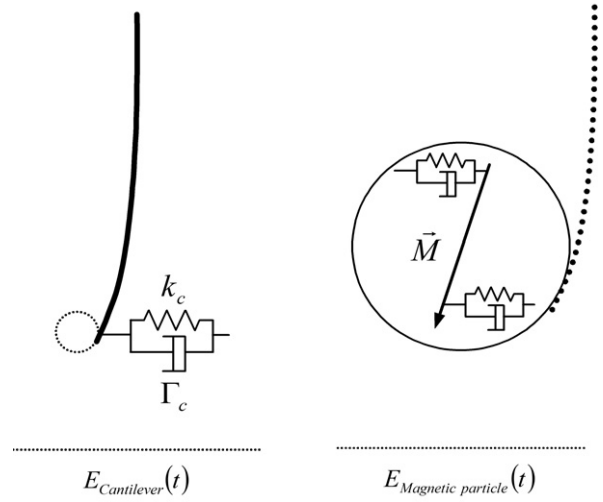


Figure 2. Cantilevers and dissipations. This sketch represents the different dampers acting on the mechanical lever. The left-hand one represents thermoelastic relaxation and the right-hand one magnetoelastic relaxation.

An independent dissipation process is also measured, when a mechanical oscillator with magnetic tip is placed in a magnetic field or interacts with a magnetic sample. There are different mechanisms by which a variable magnetic field can couple to a material and lose energy. The main loss mechanisms for magnetic materials in a magnetic field are hysteresis, conduction losses (eddy current), domain wall resonance, and electron spin resonance. The different mechanisms have diverse dependences on material properties such as sample type, microstructure, frequency and temperature.

The two effects are modelled with an independent spring and damper, where the spring is the phenomenon in phase with the change and the damper is the out-of-phase loss process. Each independent process can be added in parallel, as shown in figures 2 and 3.

The total potential energy and the losses are therefore

$$E_t = E_{\text{Cantilever}} + E_{\text{Magnetic particle}} \quad (15)$$

$$\Delta E_t = \Delta E_{\text{Cantilever}} + \Delta E_{\text{Magnetic particle}}. \quad (16)$$

The quality factor is then calculated as the ratio between total energy and loss energy per cycle.

$$Q = \frac{2\pi E_t}{\Delta E_t} = \frac{1}{\frac{1}{Q_{\text{Cantilever}}} + \frac{1}{Q_{\text{Magnetic particle}}}}. \quad (17)$$

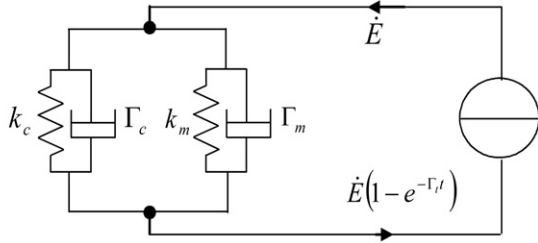


Figure 3. Energy dissipation processes. The different relaxation process are considered independent and can be added. All processes causing the dissipation energy are modelled with a spring assuming the elastic process and a damper causing the dissipation.

The quality factor contribution of each independent damping process is added in parallel. Figure 3 represents the complete system with noise excitation.

The two dissipation processes are the origin of the dephasing between excitation and detection. The dephase signal is calculated with the parameter Γ_r , which is the sum of the different dephasing processes.

1.2.1. Losses due to the oscillating magnetic field. Losses of energy are due to a change of phase between excitation and detection. A central parameter, that is used in electrodynamics, and that gives the relation between the magnetic flux and the field, is the permeability. The permeability, μ , of a material is defined by the relation $\mathbf{B} = \mu\mathbf{H} = \mu_0\mu_r\mathbf{H} = \mu_0(\mathbf{H} + \mathbf{M})$, where \mathbf{B} is the flux density (T), \mathbf{H} is the field intensity (A m⁻¹), \mathbf{M} is the magnetization (A m⁻¹), μ_0 is the permeability of free space ($4\pi \times 10^{-7}$ H m⁻¹) and μ_r the relative permeability of the material. Losses which occur in a material because of the time varying magnetic field are included in the relative permeability term by writing μ_r as a complex number, $\mu_r = \mu_{tr} - j\mu_{ri}$, where $j = \sqrt{-1}$ [6, 7].

The real term μ_{tr} describes the permeability at a fixed field without any losses. The imaginary term μ_{ri} , which describes the magnetic loss, arises from damping forces caused by internal friction during domain rotation and Bloch wall propagation.

Hysteresis losses: At low frequency this process dominates and dissipates as heat in a magnetic material as it generates a B - H hysteresis loop. The energy loss per unit sample volume is $\Delta E = \int B dH$. This loss is controlled by factors that control the low frequency permeability and coercivity such as porosity, grain size and impurity as well as the intrinsic properties. The energy used for turning the magnetization by θ_m degrees is equal to $E_a = K_1 V \sin^2 \theta_m$.

Domain wall loss: At 100 kHz the small displacements of the pinned domain wall with the applied field introduce restoring forces. The wall has inertia and its movement is accompanied by energy dissipation [9, 10]. This process due to the frequency range can be ignored.

Eddy current losses: The eddy current depends on the frequency of the varying magnetic field and the conductivity of the material. It is well known that when the skin depth $\delta = \sqrt{1/(\sigma\pi f\mu)}$ is large compared to the sample size the influence of the eddy current on the magnetic field is entirely negligible [6, 7].

The mechanical resonance frequency of the cantilever is in the kilohertz range. At room temperature the best

conductor has a penetration of 0.5 mm. This dimension is 1000 times bigger than the tip size dimension. At boiling helium temperature the skin depth of the majority of metal conductors is reduced by around 1000 times. Consequently, the use of conductors such as Ni, Co or Fe in the micron size range is affected by the eddy current. Rare earth magnets do not have a good conductivity and for this reason the eddy current can be neglected for such magnets.

The RF field excitation has a frequency of more than a gigahertz. This high frequency is still not able to cause an eddy current loss in hard magnetic materials. This high frequency can cause a severe eddy current loss in the silicon cantilever. This is the reason why the RF coil is placed parallel to the lever surface.

The energy dissipation is $\Delta E = a\sigma f^2 B^2 r^2$, where a is a constant shape dimension, σ the conductivity, f the frequency, B the magnetic field and finally r the radius of the particle.

1.2.2. Tip-field interactions. The cantilever is placed in a homogeneous static field. The vibration and the setup of the cantilever induces a small varying field, which generates a energy loss. The magnetic particle attached to the cantilever in a constant magnetic field is subjected to a variation field caused by the motion of the mechanical oscillator. It is possible to suppose the cantilever with the magnetic particle polarized in the direction of the static magnetic field and a small variation field perpendicular to this. The representation of the model is shown in figure 4.

The magnetic field \mathbf{H}_{ac} is calculated from the peak displacement x_{pk} and length l of the cantilever with the small angle assumption. The frequency ω is the frequency of the harmonic oscillator and \mathbf{M} is the magnetization of the particle.

The variation fields present inside the material induce rotation of the magnetic domains at the kilohertz range. Since the induced motions are resisted by inertial, elastic and frictional forces the response is generally a function of the applied frequency [11]. In addition to the frequency dependence the response is a function of the temperature, the magnitude of magnetic field, the orientation and the magnetic domains [11, 12].

Figure 5 represents a hypothetical hysteresis loop caused by varying the static magnetic field. The bold line shows the magnetization of the magnetic tip over the variation of the static magnetic field. Parallel to the field the process is elastic and dominated by the wall motions. Perpendicular to the magnetic field the motion is dominated by domain rotation, and small hysteresis loops are generated, causing a loss of energy. Depending on the structure, it is possible to introduce a demagnetization factor that causes a reduction of the remaining magnetic field.

The magnetic field in the particle is $\mathbf{H} = \mathbf{H}_{\parallel} + \mathbf{H}_{\perp} = \mathbf{H} \cos(\theta_m) + \mathbf{H} \sin(\theta_m) \sin(\omega t)$. In a continuous wave electron spin resonance signal the applied field is normally swept from a field \mathbf{H} parallel to the particle magnetization to a field \mathbf{H} antiparallel. This sweep causes a loss of energy marked on the left of the figure 5, but not detectable by the cantilever. In fact, the loss is not correlated with the vibration frequency of the mechanical oscillator and for this reason the Q factor is constant. This supposition is true only when

$$\text{Frequency of field sweep} \ll \text{Frequency of cantilever.}$$

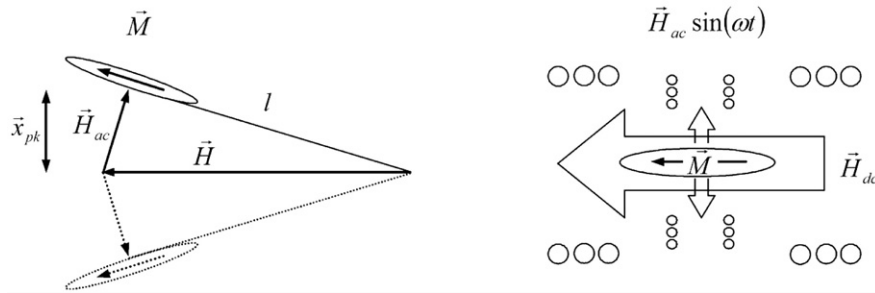


Figure 4. Tipped cantilevers in a static field. The magnetic field acting on the magnetic particle can be modelled with the sum of the axial and perpendicular components. The axial component for the low frequency sweeping can be shown as a quasistatic experiment. The perpendicular component has a frequency of oscillation of the mechanical resonator and for this reason has a strong effect on the frequency shift.

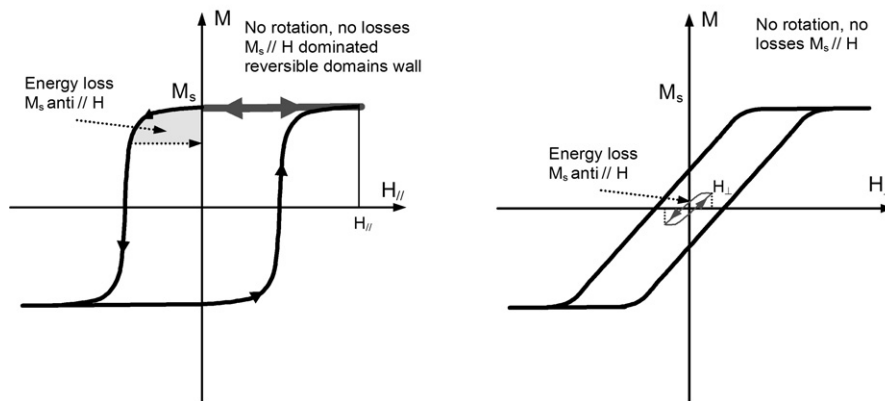


Figure 5. Hysteresis loops. The figure shows the hysteresis loop of a magnetic material. The axial components do not cause losses on the mechanical resonator, because the field is changed with a low frequency. Moreover, in the bold line part of the left graph the domains are parallel to the field and are in lower potential. The right graph shows the real cause of the dissipation: by varying the field perpendicular to the magnetic field a small loop is engendered.

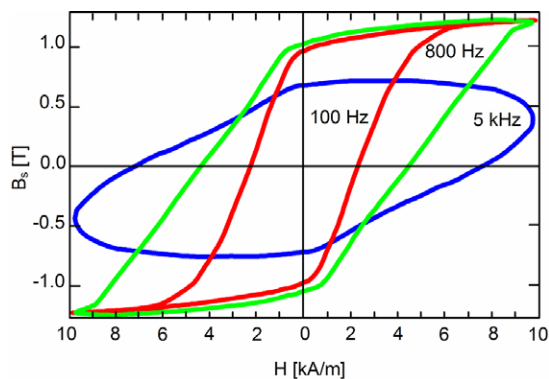


Figure 6. Hysteresis loop of FeCo. The graph represents the hysteresis loop of $\text{Fe}_{10}\text{Co}_{90}$ as a function of the frequency measured by Giri and All [13]. On the origin of the graph the change of the magnetization begins to be more difficult, because the magnetization cannot follow the fast change of the induction field. For small loops the energy dissipated is reduced with increasing frequency.

This relation demonstrates what many authors have measured [2, 3, 5], but never explained. In other words the energy loss is filtered by the mechanical resonator. The hysteresis loop is dependent on the magnetic oscillation frequency and is deformed as shown in the figure 6. The figure represents the real loop of $\text{Fe}_{10}\text{Co}_{90}$ (for the measured hysteresis loops please refer to [13]).

The more the frequency of the mechanical oscillator increases, the less the magnetic domain attached to it follows the magnetic field. This effect, which is caused by the inertia of the magnetization, consequently reduces the minor loop hysteresis and the magnetic permeability. The magnetic energy loss per cycle, which corresponds to the area of the minor loop, is then reduced.

In conclusion, at frequency lower than 1 kHz the domains follow the induced magnetic field and the maximum energy is dissipated. At higher frequency ($>1\text{--}2$ kHz) the magnetic domains due to their inertia hardly follow the magnetic field and the energy dissipated is then reduced.

1.2.3. Magnetic interaction losses. The damping measured through the Q factor provides an important parameter of the dissipation particle material and the imaginary part of the magnetic permeability. In magnetic force microscopy (MFM), one usually measures the frictional constant, which is related to the imaginary magnetic permeability. The energy magnetic loss is induced by the time varying magnetic field, which produces an amount of energy dissipation during each period. The total energy loss is extrapolated from the linear dispersive media theory of losses [6, 7]. The theory shows that at a given instant in time and space, the rate of heat generated per unit volume caused by magnetic losses is given by

$$P_{\text{losses}} = \omega \mu_0 \mu_i H_{ac}^2. \quad (18)$$

Table 2. Cantilevers and tip characteristics. The table shows the cantilevers on which a magnetic particle material has been glued. The materials are Pr₂Fe₁₄B, SmCo₅, ferrite and Nd₂Fe₁₄B. All material data are given by the magnet producer: www.Magnequench.com.

Cantilever	Nanosensor 1	Nanosensor 2	Nanosensor 3	Nanosensor 4	Nanosensor 5	IBM 1	IBM 2
Material	Pr ₂ Fe ₁₄ B	Pr ₂ Fe ₁₄ B	Pr ₂ Fe ₁₄ B	SmCo ₅	Ferrite	Nd ₂ Fe ₁₄ B	Pr ₂ Fe ₁₄ B
$\mu_0 H_c$ (T)	0.7	0.7	0.7	3.2	0.2		0.7
$\mu_0 M_s$ (T)	0.986	0.986	0.986	1.05	0.4		0.986
K_1 (MJ m ⁻³)	0.3	0.3	0.3	1.3	0.04		0.3
Mass (ng)	5	40	275	4	10	0.22	0.29
Volume (fm ³)	0.658	5.263	36.184	0.477	1.282	0.029	0.038
f_{i0} (Hz)	10734	10112	11020	10423	10523	2736	2801
f_0 (Hz)	8663.7	7321.92	3494.29	8881	8152	2158	2110
k_0 (N m ⁻¹)	0.155	0.123	0.11	0.155	0.127	0.000 14	0.000 18
Q factor	94 567	157 580	102 569	145 335	110 569	29 064	28 654
F_{\min} (N Hz ^{-1/2})	6.83×10^{-16}	5.76×10^{-16}	1.03×10^{-15}	5.45×10^{-16}	6.52×10^{-16}	7.93×10^{-17}	8.08×10^{-17}

In a complete cantilever oscillation period T , the energy dissipated by a particle with volume V is therefore

$$\Delta E = P_{\text{losses}} T = 2\pi \mu_0 \mu_i V H_{ac}^2. \quad (19)$$

The alternative magnetic field excitation can contribute to the generation of phonons and dissipate the energy by the relaxation processes through the magnetic material. This dissipated energy can be connected with the dissipated energy measured by the Q factor and the amplitude oscillation. The energy loss for a cantilever oscillating with amplitude x_{pk} is given by

$$\Delta E = \frac{2\pi E}{Q} = \frac{\pi k_0 \omega^2 x_{pk}^2}{Q \omega_0^2} = \pi \omega x_{pk}^2 \Gamma \quad (20)$$

where $\Gamma = k_0 \omega / (\omega_0^2 Q)$ represents the total friction [8]. The imaginary part of the magnetic permeability can consequently be determined by substituting the variable field H_{ac} with $H x_{pk} / l$ and by comparing equations (19), (20). The total friction and the imaginary magnetic permeability are two parameters which determinate the amount of dissipated energy. The imaginary permeability is mostly used in high frequency magnetic field instruments for calculating the energy dissipation. The MFM is a strong sensitive instrument, which can measure small variation of this parameter.

2. Experiments: tip-field interactions

In the previous section we calculated the interaction between the magnetic field and microsized magnetic particles. At small magnetic fields, a linear relation connects the magnetic field, which produces a torque on the mechanical beam, and the frequency shift. The friction and the imaginary magnetic permeability have been calculated as well. Thus, we conducted a series of experiments, in order to verify the frequency shift relation calculated in the previous section and to understand the severe energy losses while exposing the cantilever to the magnetic field.

2.1. Tip materials and setup

In this study we glued magnetic materials of various grain sizes on five Nanosensors⁴ cantilevers with a mechanical resonance

⁴ NANOSENSORS, Rue Jaquet-Droz 1, CH-2007 Neuchatel, Switzerland <http://www.nanosensors.ch>

frequency of 10 kHz and on two ultrasoft non-commercial IBM⁵ cantilevers with a mechanical resonance frequency of 2.7 kHz. The magnetic materials and cantilever characteristics are shown in table 2, before and after gluing the tip.

In order to attach the magnetic particle at the end of the ultrasoft cantilever a really minuscule quantity of optical glue⁶ was placed at the extremity of the cantilever using an optical microscope and a home-built micromanipulator. Small magnetic particles were placed on an AlO₂ substrate and scratched against an AlO₂ substrate with the purpose of reducing the dimension of the grains. After choosing the particle, the permanent magnet was mounted at the end of a cantilever.

The particle was localized and aligned with the magnetic field (it is strongly recommended not to place the magnet behind the magnetic particles, whereupon the particles become fixed and impossible to remove from the surface). After the particle was captured by the glue the cantilever was exposed to UV rays for a few hours to harden the adhesive. Finally, all cantilevers were photographed using the SEM microscope and placed in a plastic box filled with argon gas with the aim of reducing the oxidation of the magnetic particle.

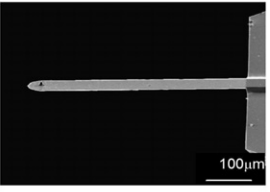
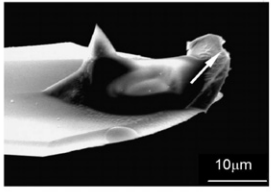
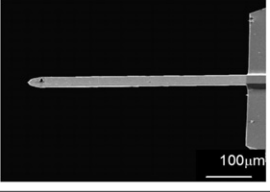
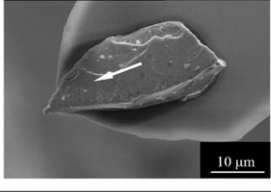
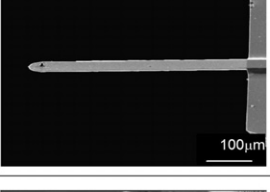
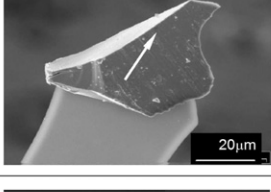
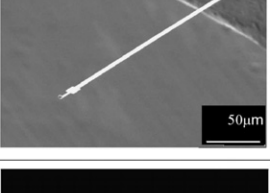
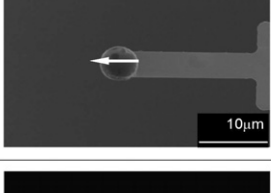
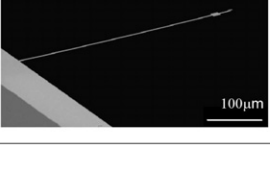
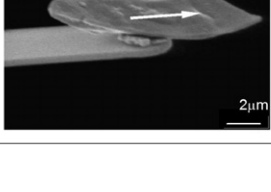
The mass of the particle attached on the cantilever was determined using the frequency shift. This is determined by the difference between the first eigenfrequency of the cantilever before attaching the magnetic particle to it, and after. The mass is then calculated. For cross validation the mass was determined by reconstructing the volume from the scanning electron microscope (SEM) pictures represented in table 3 multiplied by the mass density.

To demonstrate and measure the magnetic dissipation a dynamic mode cantilever was measured in vacuum at 10⁻⁶ mbar and at room temperature between the poles of an electromagnet (Bruker maximal magnetic field 0.5 T). The basic experiment was to measure the cantilever resonance frequency and the damping as a function of the static magnetic field. The cantilever frequency was measured with a Labview program with the FFT of a signal acquired for 30 s with a precision of 0.1 Hz, while damping was typically measured by the cantilever ring-down time after abruptly turning off the piezoelectric drive signal.

⁵ IBM Zurich, Säumerstrasse 4, CH-8803 Rüschlikon, Switzerland, <http://www.IBM.ch>

⁶ Norland optical adhesive 65, Norland Products, PO Box 637, 2540 Route 130, Suite 100, Cranbury, NJ 08512, <http://www.norlandprod.com>

Table 3. Tipped cantilevers. The table shows the cantilevers measured and their parameters, such as the resonance frequency, the spring constant, the Q factor and the minimal detection force at room temperature.

Nanosensor	Material	Pr ₂ Fe ₁₄ B		
	f ₀ [Hz]	8663.7		
	k ₀ [N/m]	0.155		
	Q	94567		
	F _{min} [N/Hz ^{0.5}]	6.8*10 ⁻¹⁶		
Nanosensor	Material	Pr ₂ Fe ₁₄ B		
	f ₀ [Hz]	7321.92		
	k ₀ [N/m]	0.123		
	Q	157580		
	F _{min} [N/Hz ^{0.5}]	5.7*10 ⁻¹⁶		
Nanosensor	Material	Pr ₂ Fe ₁₄ B		
	f ₀ [Hz]	3494.29		
	k ₀ [N/m]	0.11		
	Q	102569		
	F _{min} [N/Hz ^{0.5}]	1.0*10 ⁻¹⁵		
IBM	Material	Nd ₂ Fe ₁₄ B		
	f ₀ [Hz]	2158		
	k ₀ [N/m]	0.00014		
	Q	29064		
	F _{min} [N/Hz ^{0.5}]	7.9*10 ⁻¹⁷		
IBM	Material	Pr ₂ Fe ₁₄ B		
	f ₀ [Hz]	2110		
	k ₀ [N/m]	0.00018		
	Q	28654		
	F _{min} [N/Hz ^{0.5}]	8.1*10 ⁻¹⁷		

The measurement was repeated after the cantilever amplitude reached the steady state condition for a fixed magnetic field. The lock-in was adjusted for maximal sensitivity and the local oscillator, exciting the piezo, turned off. The measurement was repeated 30 times and then the field was changed to the next amplitude. The scheme of the equipment used for this measurement is sketched in figure 7.

2.2. The frequency shift as a function of the magnetic field

The frequency shift was measured for the cantilevers mentioned in the previous section. The frequency shift of the tipped cantilevers changes linearly with the magnetic variations. This tendency is experimentally demonstrated with various hard magnetic materials. When the anisotropy constant is larger than the product between the magnetic field and the particle magnetization, $K_1 \gg BM_s/2$ or $(D_{\perp} - D_{\parallel})\mu_0 M_s^2/2 \gg BM_s/2$, the slope can be fitted with the following linear equation:

$$\Delta\omega = \left(\frac{1}{2} \frac{\omega_0 V M_s}{k_0 l^2} \right) B - \frac{1}{8} \frac{\omega_0^3}{k_0^2} \Gamma^2. \quad (21)$$

The frequency shift depends linearly on the particle volume and its magnetization. The tipped cantilever with a hard magnetic particle is a relative magnetometer with a strong linearity for constant temperature. Since the temperature of the cantilever is not controlled the variation perturbs the measurement and causes some oscillations.

In the case when the anisotropy factor is equal to or smaller than the product between the magnetic field and the particle magnetization, the slope changes and reduces to 0. The ferrite particle shows this effect, since it has a change at 0.2 T. In this case equation (14) should be used for fitting the curve. The tabulated magnetic saturation of ferrite is at 0.4 T. So, the anisotropy constant is $K_1 = BM_s/2 = 0.04 \text{ MJ m}^{-3}$. The inflection can be used subsequently to calculate the anisotropy constant of each magnetic particle. We report the results in figure 8.

Soft materials have small anisotropy and consequently their magnetization is changed with the oscillations of the cantilever. This change causes not only a rotation of the magnetization but also a strong fluctuation field. This introduces a broadening of the change of the magnetic field

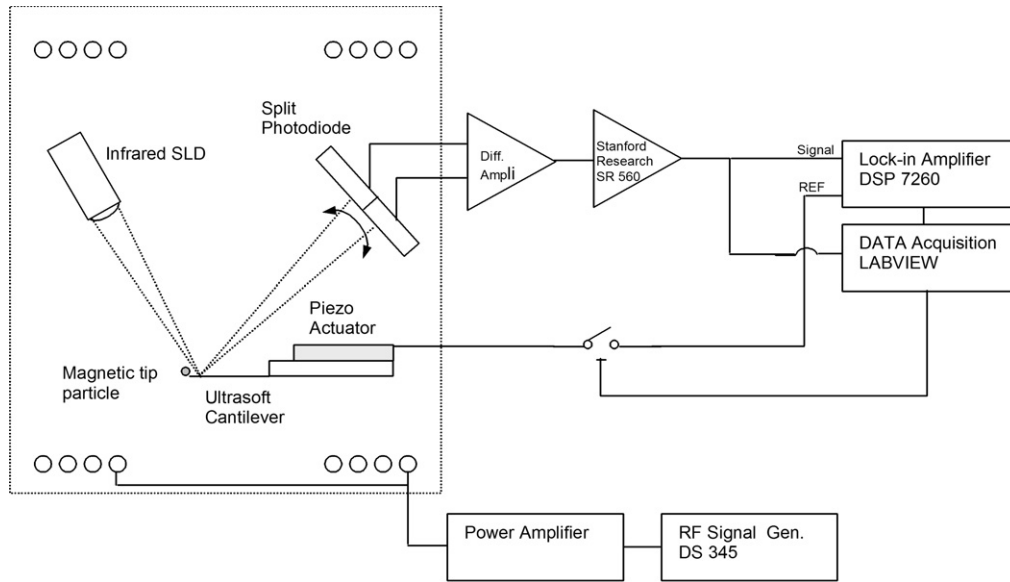


Figure 7. Tip–field interaction setup. The schematic diagram sketches the circuit used to measure the eigenfrequency and the Q factor of the cantilever with the magnetic particle. The Labview program measures the eigenfrequency of the cantilever by FFT. The lock-in is then set for the maximal sensitivity and when the oscillation of the cantilever is stable the local oscillator is turned off. The signal is measured for the decay time and repeated for different magnetic fields.

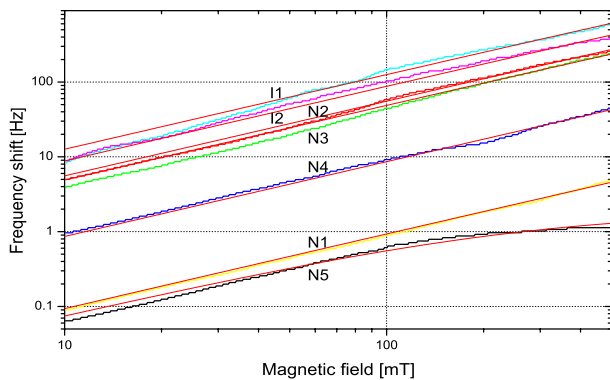


Figure 8. Frequency shift versus magnetic field. The graph shows the dependence of the frequency shift as a function of the static magnetic field applied. The labelling is the following: I stands for IBM and N stands for Nanosensors; for the numbers see table 3. All materials have a linear tendency and are fitted with equation (21). Only the ferrite N5 shows saturation and is fitted with equation (14). The change of temperature causes the perturbations.

interacting with the spins and consequently an increase of the relaxation rate spins. The magnetization of the hard material is also turned but with a smaller amplitude. For this reason, we focus our study on hard magnetic materials.

2.3. The quality factor measurement as a function of the magnetic field

In the previous section the quality factor is connected with the friction and the imaginary part of the permeability. Consequently, the Q factor is the parameter for measuring the dissipation. The quality factor of the mechanical resonator was measured using the ring-down measurement technique. Each measurement was repeated 30 times for a constant magnetic field and averaged. The data are represented in graph 9.

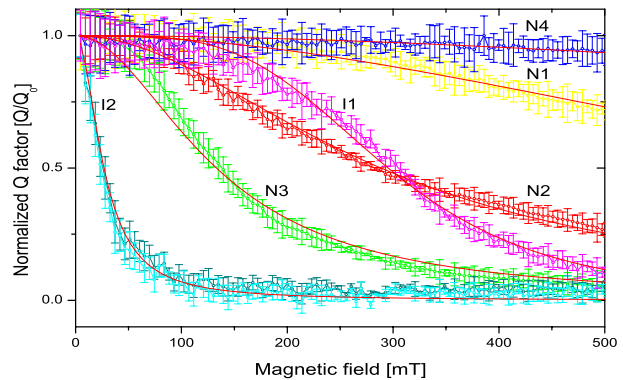


Figure 9. The graph shows the normalized Q factor of the different mechanical levers. All trends are fitted using equations (17) and (20). The Q factor can be fitted with the following equation: $Q = 1/(1/Q_0 + \omega_0^2 \Gamma / (k_0 \omega))$. The change in the Q factor is directly proportional to the volume of magnetic material glued, and inversely proportional to the anisotropy constant. The labelling is the following: I stands for IBM and N stands for Nanosensors; for numbers see table 3.

The Q factor of the cantilevers was fitted with two inelastic processes, one caused by the thermoelastic relaxation, and one caused by the tip–magnetic-field interaction. The thermoelastic relaxation is not correlated with the magnetic field. The Q factor change is directly proportional to the volume of material glued and inversely proportional to the anisotropy. The Q factor of the mechanical lever N4 does not have a strong change, because SmCo_5 has an anisotropy value 5 times larger than the anisotropy of the $\text{Pr}_2\text{Fe}_{14}\text{B}$ material glued on the cantilevers N1, N2, N3 and I2.

The magnetic friction losses for each magnetic material were extrapolated from the Q factor measurements. The magnetic friction was then divided by the volume of the

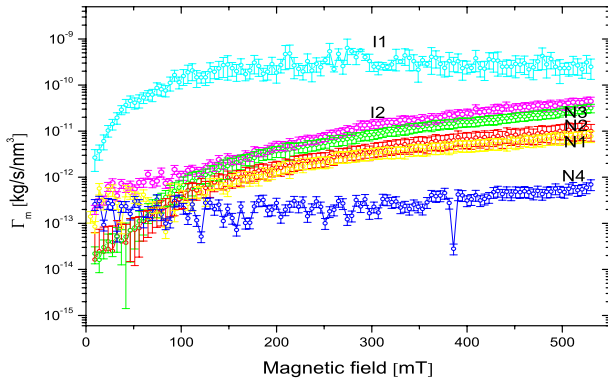


Figure 10. The graph represents the magnetic friction per nm^3 of material as a function of the magnetic field. The dissipation is correlated with the frequency. The higher the frequency the lower the dissipation. SmCo_5 has the highest anisotropy and consequently it has the lowest dissipation. The labelling is the following: I stands for IBM and N stands for Nanosensors; for numbers see table 3.

magnetic particle. The density friction can be plotted and compared. The graph 10 represents the magnetic losses per nm^3 of magnetic material. The frictional loss of the isotropic $\text{Pr}_2\text{Fe}_{14}\text{B}$ material is represented by four curves with an offset in between.

This curious effect can be explained by the frequency oscillation of the mechanical lever. In fact, as explained in the previous section the anisotropy constant is correlated with the frequency oscillation. In the case of minor loop hysteresis the energy losses are smaller, because the magnetization of the particle has inertia to turn.

The SmCo_5 has an anisotropy constant of 1.3 MJ m^{-3} , about 12 times lower than a monodomain. The large anisotropy constant may explain the constant behaviour in the range of 0.5 T. In the single spin experiment, Rugar [14] used a submicrometre magnetic tip of SmCo_5 for its incomparable anisotropy.

The vitreous $\text{Nd}_2\text{Fe}_{14}\text{B}$ spherical material has a curious strong magnetic friction that is difficult to explain. It may be attributed to the fact that the oxidation has dramatically decreased the anisotropy constant.

The magnetic frictional losses could be further decreased by reducing the particle to a monodomain dimension of $0.8 \mu\text{m}$. In this case all domain wall losses would disappear and the losses would be caused only by the hysteresis loop of the magnetic domain. The anisotropy is increased to 17 MJ m^{-3} at room temperature, to 24 MJ m^{-3} at boiling nitrogen temperature and finally to double the value at boiling helium temperature.

We know that the domains are hardly turned at higher frequency. In fact increasing the frequency causes a decrease of the magnetic friction. The data are plotted in figure 11. This behaviour is caused by the minor loop, where the field due to the frequency change is not able to turn the domains.

The friction for volume samples has a dependence on the frequency oscillation. Lower frequencies dramatically increase the dissipation due to the hysteresis effect. For frequencies higher than 10 kHz the friction is independent of the frequency [2]. The wall resonance, the eddy current and

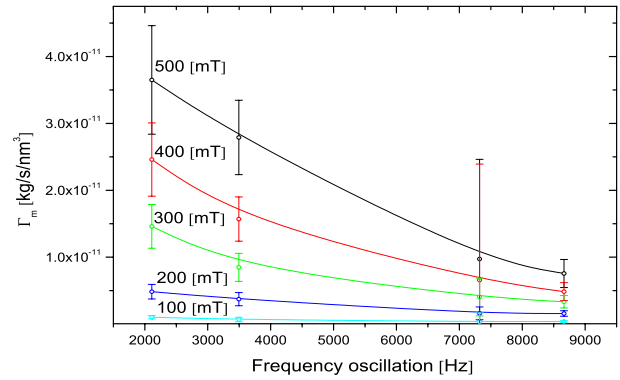


Figure 11. Magnetic friction versus frequency oscillation. The graph shows the trend of the magnetic dissipation per nm^3 as a function of the frequency of the different Nanosensors cantilevers. The trend increases at higher magnetic field.

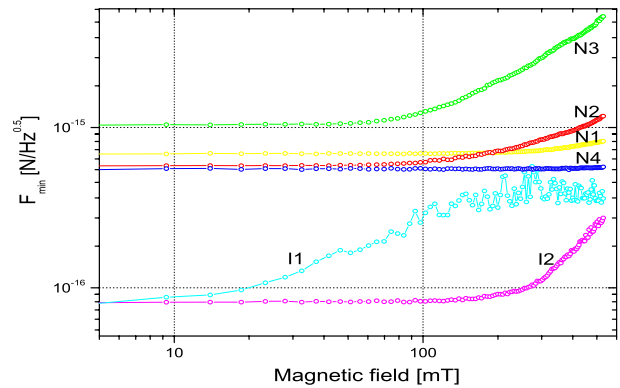


Figure 12. Sensitivity as a function of the magnetic field and Q factor. The graph shows the force sensitivity versus the magnetic field as a function of the Q factor. The spring constant and the frequency shift are supposed constant.

the electron spin resonance will increase the friction at higher frequency.

2.4. The force sensitivity as a function of the magnetic field

The force sensitivity is strongly affected by the tip–magnetic-field interaction. The choice of the right magnetic material is consequently fundamental to maintain a high sensitivity in order to measure single electron spin. The theoretical minimum measurable detecting force is given by the following equation:

$$\frac{F_{\min}}{\sqrt{\Delta f}} = \sqrt{\frac{4k_0 k_B T}{w_0 Q}} = \sqrt{4\Gamma_m m_p k_B T}. \quad (22)$$

Experimentally, it is found that the frequency shift and the spring constant hardness do not have as strong an influence on the force sensitivity as the Q factor. The force sensitivity reported in figures 12 or 13 is calculated as a function of one parameter only: either the Q factor or the spring constant. In this way, the sensitivity change can be compared. The magnetic damping loss is the major factor that reduces the force sensitivity in a static field below 0.5 T.

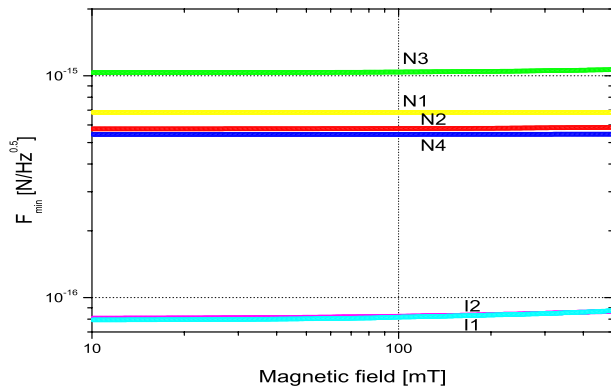


Figure 13. Sensitivity as a function of the magnetic field and frequency shift. The graph shows the force sensitivity versus the magnetic field as a function of the frequency shift and the spring constant. The Q factor is supposed constant.

A maximal sensitivity of $7.5 \times 10^{-17} \text{ N Hz}^{-1/2}$ at room temperature for the IBM cantilever is extrapolated. This force sensitivity can be increased to $9 \times 10^{-18} \text{ N Hz}^{-1/2}$ by reducing the temperature to that of boiling helium. This sensitivity is an underestimation, because the anisotropy constant increases while the temperature decreases. The same experiment should be performed at boiling helium temperature. Moreover, the sensitivity can be increased further by annealing the cantilever. In this case the grain glued at the end of the cantilever must be a monodomain in order to decrease the correlated demagnetization factor. $\text{Ne}_2\text{Fe}_{14}\text{B}$ shows a curious loss of force sensitivity for fields of more than 10 mT. $\text{Pr}_2\text{Fe}_{14}\text{B}$ and SmCo_5 have a much better behaviour and the force sensitivity holds for more than 100 mT at room temperature.

The anisotropy plays a central role in the friction process as a function of the magnetic field. In fact the sensitivity and the magnetic field range are directly correlated with the magnetic anisotropy of the particle attached to the cantilever. Low temperature and hard magnetic materials increase the magnetic anisotropy constant, which decreases the magnetic friction.

3. Conclusions: reduction damping losses

A cantilever tipped with hard magnetic materials is subjected to a severe damping losses, while exposed to a static magnetic field. A detection sensitivity of $10^{-18} \text{ N Hz}^{-1/2}$ in the absence on any magnetic field decreases to $10^{-16} \text{ N Hz}^{-1/2}$ at 100 mT. The principal cause of this sensitivity loss is due to the magnetic hysteresis loop oscillating with the frequency of the cantilever. Low frequency hysteresis changes do not have any effect on the Q factor. The hysteresis loop due to the inertia of

the magnetic domain is inversely proportional to the frequency. We find that a cantilever oscillating at 1 kHz has more magnetic losses than one oscillating at higher frequency. From the literature we can estimate that the optimal frequency oscillation is around 5–10 kHz. For a cantilever tipped with SmCo_5 or $\text{Pr}_2\text{Fe}_{14}\text{B}$, a sensitivity of $10^{-18} \text{ N Hz}^{-1/2}$ is maintained constant up to 100 mT. This sensitivity should be enough for a single electron spin detection experiment.

Acknowledgments

This work was supported by the national program TopNano 21, and the National Center of Competence in Research on Nanoscale Science (NCCR). We thank J-P Ramseyer for the SEM images.

References

- [1] Gysin U 2002 Temperaturverhalten der Elastizität und inneren Reibung mikromechanischer Resonatoren *Thesis* Basel
- [2] Stipe B C, Mamin H J, Stowe T D, Kenny T W and Rugar D 2001 Magnetic dissipation and fluctuation in individual nanomagnets measured by ultrasensitive cantilever magnetometry *Phys. Rev. Lett.* **86** (13)
- [3] Marohn J, Faichtein R and Smith D D 1998 An optimal magnetic tip configuration for magnetic-resonance force microscopy of microscale buried features *Appl. Phys. Lett.* **73** (25)
- [4] Skomski R and Coey J M D 1999 *Permanent Magnetism* (Bristol: Institute of Physics Publishing)
- [5] Zhang Z and Hammel P C 1998 Magnetic force microscopy with ferromagnetic tip mounted on the force detector *Solid State Nucl. Magn. Reson.* **11** 65–72
- [6] Jackson J D 1999 *Classical Electrodynamics* (New York: Wiley)
- [7] Landau L D, Lifshitz E M and Pitaevskii L P 2004 *Electrodynamics of Continuous Media* (Woburn, MA: Butterworth–Heinemann)
- [8] Stipe B C, Mamin H J, Stowe T D, Kenny T W and Rugar D 2001 Noncontact friction and force fluctuations between closely space bodies *Phys. Rev. Lett.* **87** (9)
- [9] Grütter P, Liu Y and LeBlanc 1997 Magnetic dissipation force microscopy *Appl. Phys. Lett.* **71** (2)
- [10] Liu Y, Ellman B and Grütter P 1997 Theory of magnetic dissipation imaging *Appl. Phys. Lett.* **71** (8)
- [11] Krage M 1981 Microwave sintering of ferrites *Ceram. Bull.* **60** (11)
- [12] McHenry M E and Laughlin D E 2000 *Nano-Scale Materials Development for Future Magnetic Applications* vol 48 (Amsterdam: Elsevier Science)
- [13] Giri A, Chowdary K M and Majetich S A 2000 AC magnetic properties of compound FeCo nanocomposites *Mater. Phys. Mech.* **1** 1–10
- [14] Rugar D, Budakian R, Mamin H J and Chui B W 2004 Single spin detection by magnetic resonance force microscopy *Nature* **430** (July)